

OPEN ACCESS

Stud arc welding in a magnetic field – Investigation of the influences on the arc motion

To cite this article: K Hartz-Behrend *et al* 2014 *J. Phys.: Conf. Ser.* **550** 012003

View the [article online](#) for updates and enhancements.

You may also like

- [A metrological approach for the calibration of force transducers with interferometric readout](#)
S V Beekmans and D Iannuzzi
- [THE MANGA INTEGRAL FIELD UNIT FIBER FEED SYSTEM FOR THE SLOAN 2.5 M TELESCOPE](#)
N. Drory, N. MacDonald, M. A. Bershadly et al.
- [Temperature insensitive low-loss optical connection for automotive qiqabit plastic optical fiber communication](#)
Masahiro Uchida, Hiroshi Tanaka, Shigeru Kobayashi et al.

Stud arc welding in a magnetic field – Investigation of the influences on the arc motion

K Hartz-Behrend¹, J L Marqués², G Forster¹, A Jenicek³,
M Müller³, H Cramer³, A Jilg⁴, H Soyer⁴ and J Schein¹

¹ Universität der Bundeswehr München, Institut für Plasmatechnik und Mathematik, Neubiberg, Germany

² Universität der Bundeswehr München, Institut für Automatisierungs- und Regelungstechnik, Neubiberg, Germany

³ GSI mbH, Niederlassung SLV München, München, Germany

⁴ Heinz Soyer Bolzenschweisstechnik GmbH, Wörthsee, Germany

E-mail: karsten.hartz-behrend@unibw.de

Abstract. Stud arc welding is widely used in the construction industry. For welding of studs with a diameter larger than 14 mm a ceramic ferrule is usually necessary in order to protect the weld pool. Disadvantages of using such a ferrule are that more metal is molten than necessary for a high quality welded joint and that the ferrule is a consumable generally thrown away after the welding operation. Investigations show that the ferrule can be omitted when the welding is carried out in a radially symmetric magnetic field within a shielding gas atmosphere. Due to the Lorentz force the arc is laterally shifted so that a very uniform and controlled melting of the stud contact surface as well as of the work piece can be achieved. In this paper a simplified physical model is presented describing how the parameters welding current, flux density of the magnetic field, radius of the arc and mass density of the shielding gas influence the velocity of the arc motion. The resulting equation is subsequently verified by comparing it to optical measurements of the arc motion. The proposed model can be used to optimize the required field distribution for the magnetic field stud welding process.

1. Introduction

Stud arc welding, also called stud welding, is an arc welding process in which a metal fastener (stud) is welded onto a metal work piece. It is a welding process widely used in the construction industry [1]. The type of arc ignition, the welding duration, the weld pool shielding and the type of power source define different process types [2]. In this paper the drawn-arc stud welding process with a ceramic ferrule will be considered. In general, the use of a ceramic ferrule is necessary when studs with a diameter larger than 14 mm are to be welded. The ceramic ferrule is used for protecting the weld pool but the application of a ferrule has the disadvantage that more metal is molten than necessary for a high quality welded joint, i.e. the energy load during the welding process is higher than required. Additionally the ferrule is a consumable usually thrown away after the welding operation and thus it would be an advantage if the ferrule could be omitted.

About 5 years ago a new process form of stud welding was presented: radially symmetric magnetic field stud welding. In this process a radially symmetric magnetic field is used to laterally shift the arc by means of the Lorentz force such a way that a very uniform and controlled melting of the stud and



the work piece can be achieved [3]. Main advantages of this new process variant are that the ceramic ferrule can be omitted [3] and that the energy load is reduced by about 70 percent, resulting in lower thermal stress inside the work piece and therewith a reduced work piece distortion. By means of radially symmetric magnetic field stud welding it is possible to weld studs with a diameter larger than 12 mm. High quality welded joints for studs with a diameter of 16 mm have been achieved.

The aim of this paper is to present a simplified theoretical model describing the effect of important process parameters in the magnetic field stud welding process on the velocity of the arc motion. Such a model can be very useful for both modeling and optimizing the magnetic field stud welding process. The equation resulting from this model agrees quite well with optical measurements of the arc motion.

The paper is organized as follows: In the next two sections the conventional stud welding process and the magnetic field stud welding process without ferrule are described. In the section that follows a simplified physical model for the arc motion under a magnetic field is derived. In order to experimentally verify the resulting equations an optical measurement setup has been developed, as described in the fifth section. In the last section the experimental results as well as their good agreement with the theoretical model is discussed. The paper concludes with a summary and an outlook.

2. Drawn-arc stud welding with a ceramic ferrule

The drawn-arc stud welding process with a ceramic ferrule consists of four steps (figure 1):

- In the first step, a stud is loaded into the chuck of a welding gun, a ceramic ferrule is placed around the stud, and the stud is positioned against the work piece to close an electrical circuit with a current of about 100 A.
- Afterwards a trigger is pressed and the welding gun lifts up the stud in the ceramic ferrule. An initial pilot arc is ignited, creating an electric path for the welding current. After a short fixed time of about 100 ms the actual welding electric current is switched on and the resulting welding arc melts the stud surface as well as the work piece.
- During step three the stud is plunged into the molten weld pool.
- Finally the welding is completed and the welding gun is lifted off. The ferrule is mechanically removed.

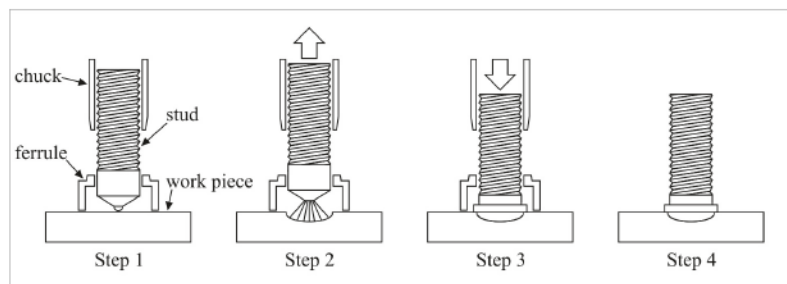


Figure 1. The four steps of a drawn-arc stud welding process

In the next section the magnetic field stud welding process is described, as well as its differences to the welding process just described in this section.

3. Magnetic field stud welding

For the magnetic field stud welding process no ceramic ferrule is used. In order to protect the weld pool a shielding cap is surrounding the welding area (figure 2). This cap is automatically lowered once a trigger has been pressed and subsequently a shielding gas is introduced into the cap. After a fixed period of time the stud is lifted up and a pilot arc is ignited. The process steps following the lifting of the stud are similar to those for the welding process with a ferrule, the only difference being the applied magnetic field. This field is generated by an electric coil located in the shielding cap. Due to

the magnetic field a Lorentz force is acting perpendicularly on the arc resulting in a lateral arc motion. As already mentioned a very uniform and controlled melting of the stud surface and the work piece can be achieved due to this arc motion.

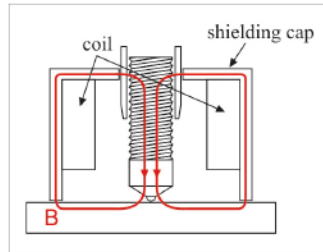


Figure 2. Principle of magnetic stud welding

4. A simplified theoretical model for the magnetic field stud welding

In order to model and/or optimize the magnetic field stud welding process it is very helpful to assess the arc motion as a function of the most relevant process parameters. In this section a simplified model is presented which allows to correlate the velocity of the arc motion to such parameters as welding current, applied magnetic field, arc radial extension and mass density of the cold shielding gas. Let us consider a vertical plasma cylinder of constant radius r_{core} , carrying a stationary electric current I_{el} directed upwards (figure 3). We assume in a first approximation that the whole cylinder displays a homogeneously constant temperature and that the electric current is also homogeneously distributed across the cylinder cross section such that the resulting electric current density within the plasma core is equal to

$$j_{el} = \frac{I_{el}}{\pi r_{core}^2}. \quad (1)$$

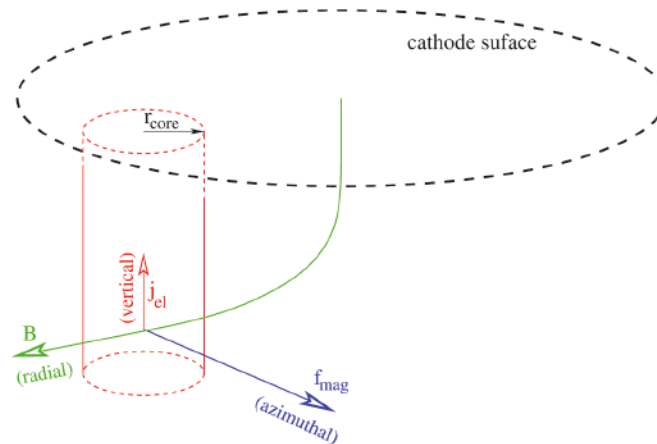


Figure 3. Lateral Lorentz force f_{mag} acting on a vertical plasma cylinder

The cathode spot of this plasma column is located at some off-center position at the cathode surface and a stationary magnetic field B produced by the coil displays a mainly radial component at the lower part of the plasma column, pointing outwards (see figure 3). As a result a magnetic force per volume of magnitude

$$f_{mag} = j_{el} B \quad (2)$$

is produced in azimuthal direction, dragging tangentially the plasma core and generating thus an approximately circular motion of the plasma column. The mechanical work W spent during a core displacement of r_{core} to a position where previously only surrounding cold shielding gas existed leads to the following relation for the work per volume:

$$\frac{W}{Volume} = f_{mag} r_{core} = j_{el} B r_{core} \quad (3)$$

The main contribution to W arises from the displacement of the more massive cold shielding gas volume surrounding the plasma column. Thus the mechanical work (per volume) mainly goes into an increase in kinetic energy (per volume) to the final arc velocity v_{arc} . This can be expressed by

$$j_{el} B r_{core} \approx \frac{1}{2} \rho_{gas}(T_{cold}) v_{arc}^2 \Rightarrow v_{arc} \approx \sqrt{\frac{2 I_{el} B}{\pi r_{core} \rho_{gas}(T_{cold})}} \quad (4)$$

or equivalently

$$v_{arc}^2 \propto \frac{I_{el} B}{r_{core} \rho_{gas}(T_{cold})}, \quad (5)$$

whereas $\rho_{gas}(T_{cold})$ represents the mass density of the cold shielding gas. A more detailed derivation of a similar relation can be found in [4]. It is worth noting that the simple model leading to equation (4) does not include the partial heating of some peripheral regions of the plasma column, produced by the electric current across the plasma core and required for its existence. Hence the kinetic energy variation of the plasma core actually contains an additional contribution depending on the temperature of the plasma column but independent of the applied magnetic field. Furthermore the magnetic tangential force particularly acts on the lower part of the plasma core, slightly bending the plasma column and producing thus an additional radial component in the arc motion.

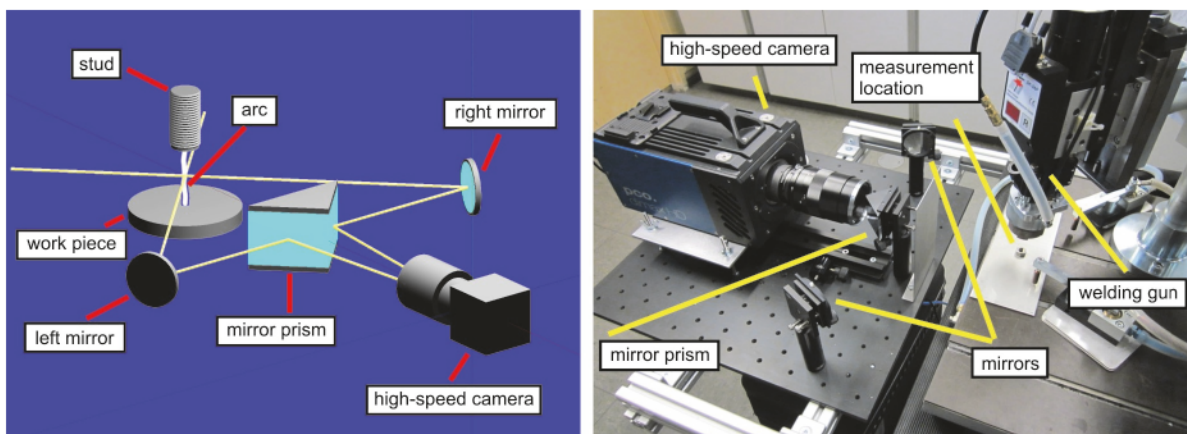


Figure 4. High-speed stereo optical system (left: measuring principle; right: experimental setup)

Since the derivation of the relations (4) and (5) is based on several simplifying assumptions about the plasma arc, it should be verified if these relations also hold for a real magnetic field stud welding process. The experimental verification of equation (5) is carried out by means of a high-speed stereo optical investigation of the arc motion, as presented in the next section.

5. Description of the high-speed stereo optical setup

In the developed experimental setup, the moving arc is observed at an angle of 90° by using 2 mirrors and a mirror prism (figure 4). By means of the mirror prism, the 2 images of the arc are projected

simultaneously onto the CCD-chip of a high-speed camera (model “dimax HD” from the company PCO). Due to the different viewing angle in the 2 images the arc position can be determined. Two typical examples of the recorded measurements are given in figure 5: initial ignition of the pilot arc (above) and full developed welding arc (below). (above) and full developed welding arc (below).



Figure 5. Stereo optical arc images during the magnetic field stud welding process (above: ignition of pilot arc; below: actual welding arc; left/right: images obtained with the left/right mirror of the stereo optical system). The dotted lines indicate the position of the stud and the work piece, respectively.

6. Investigation of the arc motion by means of high-speed stereo optical setup

In this section the experimental results for the arc motion and their agreement with the theoretical model are discussed. During the experiments the arc was recorded at a frame rate of 10,000 fps and a resolution of 960x100 pixels. The exposure time was set at 2 μ s. For each investigated parameter the measurement was repeated 3 times. The mean arc motion velocity \bar{v}_{arc} is determined by averaging the position change of the arc between two consecutive images. Studs of diameter 12 mm and 16 mm were used, with a two-component shielding gas mixture comprising 82 % argon and 18 % carbon dioxide (Corgon 18). First, the welding current I_{el} was set to 600 A, 800 A, 1000 A and 1200 A, with a constant coil current of 705 mA and studs with a diameter of 16 mm. In this case the recorded images of the high-speed camera were used to determine both the arc position as well as the mean radial extension \bar{r}_{bright} of the bright area of the welding arc. This latter radius is directly proportional to actual radius \bar{r}_{core} of the plasma arc.

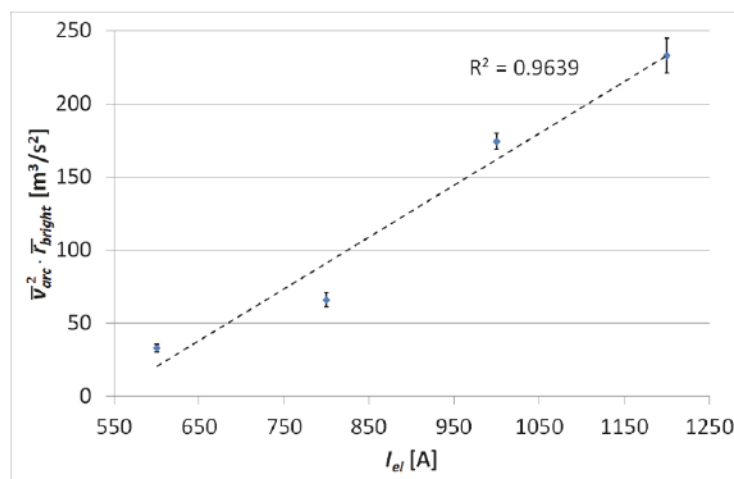


Figure 6. Nearly linear increase with the welding current I_{el} of the squared mean velocity of the arc motion \bar{v}_{arc}^2 , multiplied with the radial extension \bar{r}_{bright} of the bright area of the welding arc (proportional to the mean radius \bar{r}_{core} of the arc). Each measurement point corresponds to the mean value of three measurements and the error bars indicate one standard deviation from that mean value.

As displayed in figure 6 there exists a very good linear correlation between the squared arc velocity multiplied by the \bar{v}_{bright} and the electric current flowing through the arc:

$$\bar{v}_{arc}^2 \cdot \bar{v}_{bright} \propto I_{el} . \quad (6)$$

Hence

$$\bar{v}_{arc}^2 \propto \frac{I_{el}}{\bar{v}_{core}} \quad (7)$$

just as expected from the simplified theoretical model. The vertical offset of the straight line shown in figure 6 is related to the additional contribution to the kinetic energy density discussed at the end of the previous section. In figure 6 the standard deviation at each measurement point is between 3 and 7 percent of \bar{v}_{arc}^2 , multiplied with \bar{v}_{bright} .

In a second experimental investigation the applied magnetic field was modified by selecting the coil current I_{coil} to 210 mA, 330 mA, 450 mA, 1100 mA and 1500 mA. The welding current I_{el} was kept constant at a value of 700 A and studs with a diameter of 12 mm were used. As shown in figure 7 the following linear relation

$$\bar{v}_{arc}^2 \propto I_{coil} \quad (8)$$

holds in a good approximation. Since the strength of the horizontally applied magnetic field B in the gap between the stud and the work piece is proportional to the coil current I_{coil} we conclude

$$\bar{v}_{arc}^2 \propto B , \quad (9)$$

which corresponds to the equation derived in the simplified model. In figure 7 the standard deviation at each measurement point is between 7 and 13 percent of \bar{v}_{arc}^2 .

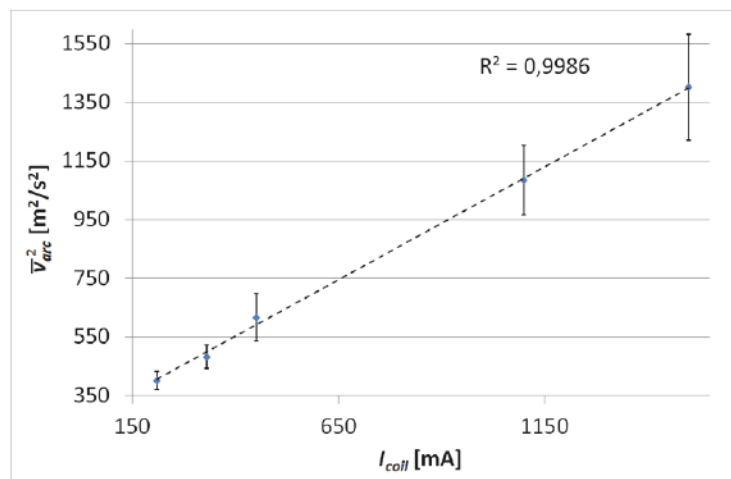


Figure 7. Nearly linear increase with the coil current I_{coil} of the squared mean velocity of the arc motion \bar{v}_{arc}^2 . Each measurement point corresponds to the mean value of three measurements and the error bars indicate one standard deviation from that mean value.

In order to investigate the influence of the shielding gas density on the velocity of the arc motion stud welding experiments with helium as shielding gas were performed. The ratio of density between

Corgon 18 and helium is approximately a factor of 10. Due to relation (5) for the mean velocity \bar{v}_{arc} of the arc motion a difference of approximately a factor 3 can be expected. The experiments display an average arc velocity of $\bar{v}_{arc} = 22$ m/s for Corgon 18 and $\bar{v}_{arc} = 65$ m/s for helium, with constant arc welding current of $I_{el} = 700$ A and coil current of $I_{coil} = 330$ mA. This is again in good agreement with the theoretical model.

7. Summary and outlook

In this paper the magnetic field stud welding process has been investigated. The main advantage of this welding process, compared to a process using a ceramic ferrule, is that this consumable ferrule can be omitted. As a consequence the energy load is reduced, less metal is molten and the thermal stress induced in the work piece is reduced. Based on a physical theoretical model a simple equation has been derived relating the motion velocity of the welding arc to parameters such as welding current, flux density of the applied magnetic field, radius of the arc and mass density of the shielding gas. This equation has been experimentally verified by recording the arc motion with a high-speed stereo camera. Such equation can be useful for both modeling and optimizing the magnetic field stud welding process. In future work a detailed simulation of the local magnetic field distribution will be carried out in order to determine how the geometry of the welding gun and coil influence the motion of the welding arc.

Acknowledgements

This work is funded by the Bayerische Forschungsstiftung BFS (Bavarian Research Foundation), funding number AZ 959-11. This support is gratefully acknowledged.

References

- [1] Chambers H A 2001 *PCI journal* **46** 46
- [2] Jenicek A and Cramer H 2003 *Welding and Cutting* **55** 105
- [3] Jenicek A, Forster G, Hartz-Behrend K, Müller M, Reiter T, Schein J and Soyer H 2013 Reproduzierbare Schweissqualität durch Bolzenschweißen mit Hubzuendung und magnetisch bewegtem Lichtbogen *DVS Congress 2013, DVS-Berichte Band* **296** 289
- [4] Maecker H H and Stablein H G 1986 *IEEE Transactions on Plasma Science* **PS-14** 291